

# Principle of Flexible Ground-Fault Arc Suppression Device Based on Zero-Sequence Voltage Regulation

**BISHUANG FAN<sup>1</sup>, (Member, IEEE), GANZHOU YAO<sup>1</sup>, (Student Member, IEEE),  
KUN YU<sup>1</sup>, (Member, IEEE), XIANGJUN ZENG<sup>1</sup>, (Senior Member, IEEE),  
WEN WANG<sup>1</sup>, (Member, IEEE), CHAO ZHUO<sup>1</sup>, AND JOSEP M. GUERRERO<sup>2</sup>, (Fellow, IEEE)**

<sup>1</sup>School of Electrical and Information Engineering, Changsha University of Science & Technology, Changsha 410114, China

<sup>2</sup>Department of Energy Technology, Aalborg University, 9100 Aalborg, Denmark

Corresponding author: Kun Yu (kuny0707@163.com)


This work was supported by the National Science and Technology Project (Research on Fundamental Theory of Safe Operation with Grounding Fault Phase Voltage Actively Reduced for Neutral Ineffectively Grounded System) under Grant 51807012 and (Research on Coordinated Control methods of Single-Phase-to-Ground Fault Flexible Arc Suppression and Protection for Distribution Networks) Grant 51877011.

**ABSTRACT** Single-line-to-ground (SLG) fault arcs cause the intermittent over-voltages, leading to short circuits within large-scale area. In this paper, a flexible arc suppression device is proposed, which adopts a zigzag grounding transformer, multi-terminal breakers and an isolation transformer to regulate zero-sequence voltage. Principle of zero-sequence voltage regulation (ZVR) and arc suppression method is presented. By carefully choosing the secondary side voltages of grounding transformer as the input of isolation transformer, the zero-sequence voltage is nearly constrained to the opposite of faulty phase supply voltage, and the ground-fault current is limited to a very small value. This device has high adaptability for low-resistance ground fault as it doesn't adopt any electronic apparatus. A 10kV prototype was established and multiple fault conditions were experimented to verify the effectiveness of the proposed ZVR device and its arc suppression principle.

**INDEX TERMS** Distribution networks, ground-fault, arc suppression, SLG fault, zero-sequence voltage regulation.

## I. INTRODUCTION

In power system distribution network, most of the reliability problems originate from single-line-to-ground (SLG) fault. If the capacitive current exceeds a certain range, the grounding arc will not self-extinguish. The intermittent arc may bring about phase over-voltage, line-to-line faults and insulation failure [1]. Additionally, the grounded electrified wire will threaten livestock and human-beings' safety, or ignite the shrubs, which may endanger public and personnel safety, causing serious social impacts and economic losses [2]. To constrain the SLG fault current, resonant grounded systems have been adopted in China and Europe [3], [4], and the ability of total fault current elimination is emphasized in practice [5].

The associate editor coordinating the review of this manuscript and approving it for publication was Ali Raza .

There are two major fault current elimination methods: the current-controlled method and the voltage-controlled method. The current-controlled methods, such as Peterson coil and the current-controlled inverter, depend on the measurement of the distributed parameters to compensate the capacitive current [6]–[10]. The effect of current compensation lies on the measurement accuracy of distributed parameters [11], [12]. The voltage-controlled methods, such as the voltage-controlled inverter, limit the fault current by forcing the neutral-to-ground voltage to be the opposite of the faulty phase supply voltage without the measurement of the distributed parameters [13]–[15]. However, the inverter-based active arc suppression device (ASD) faces overload capability, high cost, and reliability problems [16]–[20].

A passive voltage-controlled ASD to regulate the zero-sequence voltage is proposed in this paper. It is composed of a zigzag grounding transformer, multi-terminal breakers, and

a single-phase isolation transformer. The zero-sequence voltage can be easily constrained to be the opposite of the faulty phase supply voltage, only by switching the multi-terminal breakers and adjusting the number of turns in transformers.

The rest of the paper is organized as follows. In Section II, the principle of zero-sequence voltage regulation and arc suppression method of the proposed arc suppression device is presented. In Section III, a fault model of typical non-effective neutral 10KV distribution network was established and multiple fault conditions were simulated, followed by the arc suppression flowchart. In Section IV and V, simulation and experimental results are presented to verify the effectiveness of the proposed device.

## II. PRINCIPLE OF THE PROPOSED ARC SUPPRESSION DEVICE

A passive voltage-controlled ASD with a typical non-effective grounded 10kV distribution network topology is presented, as shown in Fig. 1.

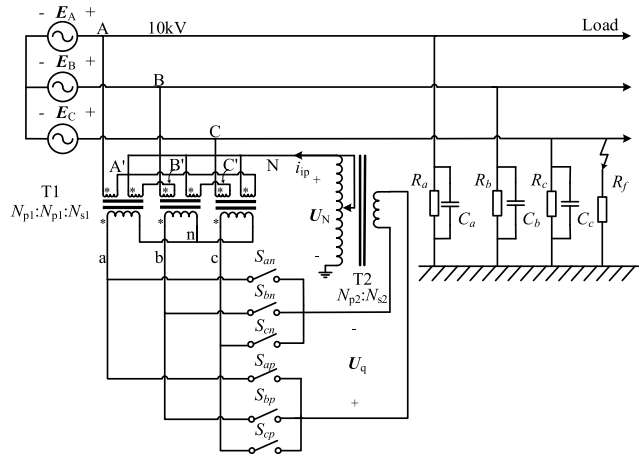


FIGURE 1. Topology of distribution network.

A zigzag grounding transformer ( $T_1$ ) is adopted to form the neutral point. It is of the connection type Zny11. A single-phase isolated transformer ( $T_2$ ) is adopted to inject a voltage to the neutral point for the purpose of arc suppression. The secondary sides of both the transformers are connected by six breakers ( $S_{an}$ ,  $S_{bn}$ ,  $S_{cn}$ ,  $S_{ap}$ ,  $S_{bp}$ ,  $S_{cp}$ ) which are used to choose suitable line-to-line voltages for the injected neutral voltage.

The turns of primary (high-voltage side) winding of  $T_2$  are adjustable to change the injected voltage in case the bus voltage changes.  $U_{AA'}$ ,  $U_{BB'}$  and  $U_{CC'}$  are the voltages of the primary main windings of  $T_1$ .  $U_{A'N}$ ,  $U_{B'N}$  and  $U_{C'N}$  are voltages of the primary side phase-shift windings of  $T_1$ .  $u_a$ ,  $u_b$  and  $u_c$  are voltages of the secondary side windings of  $T_1$ .  $E_A$ ,  $E_B$ , and  $E_C$  are the three-phase supply voltages. Both the main and phase-shift windings have the turn number of  $N_{p1}$ . The secondary winding has the turn number of  $N_{s1}$ . The turn number of the primary and secondary side of  $T_2$  are  $N_{p2}$  and  $N_{s2}$ , respectively. Fig. 2 shows the voltage phasor diagram of the transformer  $T_1$ .

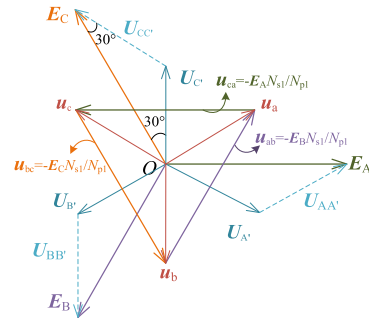


FIGURE 2. Voltage vector diagram of high-voltage side and low-voltage side of zigzag grounding transformer.

The relationship between  $U_{bc}$ , and  $E_C$  can be obtained as follows.

$$\frac{U_{bc}}{E_C} = \left| \frac{U_{bc}}{u_c} \frac{u_c}{U_{CC'}} \frac{U_{CC'}}{E_C} \right| e^{j\pi} = \sqrt{3} \frac{N_{s1}}{N_{p1}} \frac{1}{\sqrt{3}} e^{j\pi} = \frac{N_{s1}}{N_{p1}} e^{j\pi} \quad (1)$$

Similarly, the line-to-line voltage  $u_{ca}$  is the opposite of the phase-A supply voltage  $E_A$  times  $N_{s1}/N_{p1}$ . The line-to-line voltage  $u_{ab}$  is the opposite of  $E_B$  times  $N_{s1}/N_{p1}$ . The  $e^{j\pi}$  denotes  $(\cos \pi + j \sin \pi)$ . The relationship of the primary and secondary winding voltages of  $T_2$  is

$$\frac{U_N}{u_q} = \frac{N_{p2}}{N_{s2}} \quad (2)$$

When the SLG fault happens, (e.g., phase C) [21], ZVR arc suppression device functions, then a set of breakers  $S_{bn}$  and  $S_{cp}$  are turned on to generate the line-to-line voltage  $u_{bc}$  as the input of the secondary-side in the single-phase isolated transformer ( $T_2$ ),  $u_q$ .

Therefore, the neutral voltage can be constrained to

$$U_N = \frac{N_{p2}}{N_{s2}} \frac{N_{s1}}{N_{p1}} E_C e^{j\pi} \quad (3)$$

Therefore, if the turn ratio of  $T_2$  meets

$$\frac{N_{p2}}{N_{s2}} = \frac{N_{p1}}{N_{s1}} \quad (4)$$

$U_N$  would be the opposite of  $E_C$  or

$$U_N = E_C e^{j\pi} \quad (5)$$

Therefore, the faulty phase voltage and the ground-fault current would be zero, which derives the basic arc suppression principle of the proposed device.

Similarly, if the faulty phase is phase A, the breakers  $S_{an}$ ,  $S_{cp}$  are turned on to force  $u_q$  to be the line-to-line voltage  $u_{ca}$ . If the faulty phase is phase B, the breakers  $S_{bn}$ ,  $S_{ap}$  are turned on to force  $u_q$  to be the line-to-line voltage  $u_{ab}$ . The switch logic of multi-terminal breakers is listed in TABLE 1 and the speed of multi-terminal breakers is tested as milliseconds' level.

TABLE 1. True value of switch for line-to-line voltages.

Voltage $u_q$	$S_{an}$	$S_{bn}$	$S_{cn}$	$S_{ap}$	$S_{bp}$	$S_{cp}$	Faulty phase
$u_{ca}$	1	0	0	0	0	1	Phase A
$u_{ab}$	0	1	0	1	0	0	Phase B
$u_{bc}$	0	0	1	0	1	0	Phase C

### III. ZERO-SEQUENCE VOLTAGE REGULATION METHOD

In the construction of the topology shown in Fig. 1,  $u_{ab}$ ,  $u_{bc}$  and  $u_{ca}$  are the input of the secondary-side in the transformer  $T_2$ , which is equivalent as voltage  $u_q$ , thus the simplified distribution network is shown in Fig. 3. The line-to-line voltage  $u_q$  is treated as an ideal voltage source supplying the secondary-side of  $T_2$ . The distributed parameters of the transmission line are assumed to be symmetrical.  $C_0$  is the line-to-ground capacitance and  $R_0$  is the line-to-ground leakage resistance. The primary turns  $N_{p2}$  of  $T_2$  are changeable for precise control of the neutral voltage.  $N_{p2-sum}$  is the total number of turns in primary-side of  $T_2$ .  $i_{ip}$  is the injected current to the neutral point.  $I_q$  is the current from the secondary-side of the single-phase isolation transformer  $T_2$ .

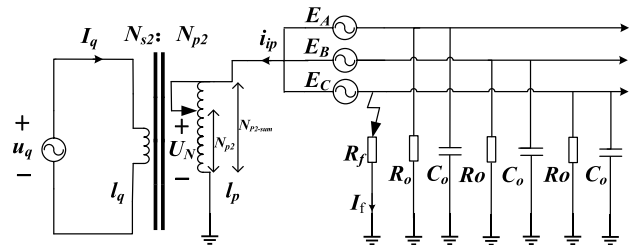


FIGURE 3. Simplified distribution network.

Assuming the two transformers are completely under control, then the grounding system can be treated as an ideal zero-sequence voltage source as shown in Fig. 4. With the consideration of the leakage inductances in both transformers  $T_1$  and  $T_2$ , the distribution network can be simplified to a voltage source in series with the leakage inductances.

We assume SLG fault happens in phase C, then the circuit of the whole system of Fig. 1 can be simplified to Fig. 4, where  $Z_\Sigma$  denotes the impedance of the distribution network and is shown in (6), where  $Y_X$  is the phase-to-ground admittance, i.e.,  $Y_X = j\omega_0 C_X + 1/R_X$  ( $X = A, B$  or  $C$ ) and  $\omega_0$  denotes the fundamental angular frequency.

$$Z_\Sigma = \frac{1}{Y_\Sigma} = \frac{1}{Y_A + Y_B + Y_C} \quad (6)$$

$l_{lk-T1}$  and  $l_{lk-T2}$  are the leakage inductances of  $T_1$  and  $T_2$ , respectively. From Fig. 4(b), the neutral voltage for suppressing the fault arcs can be obtained by assuming that the fault current is equal to zero.

$$U_N = -E_C \left( 1 + j3\omega_0 \frac{l_{lk-T1} + 3l_{lk-T2}}{Z_\Sigma} \right) \quad (7)$$

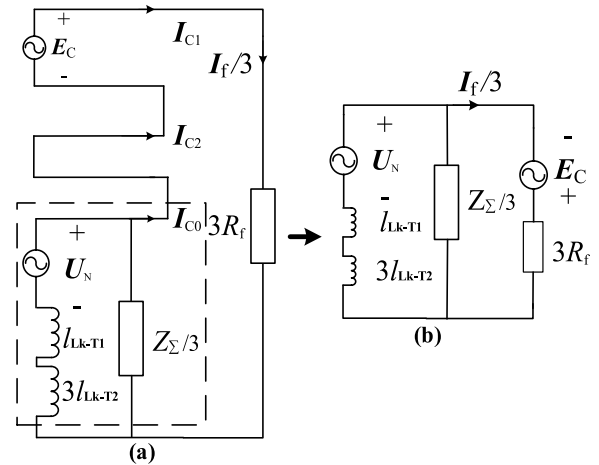


FIGURE 4. Zero-sequence simplified distribution network.

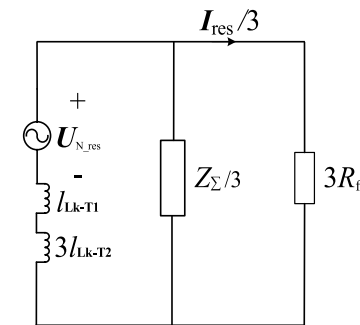


FIGURE 5. Zero-sequence simplified distribution network for residual fault current calculation.

As the distributed parameter  $G_\Sigma$  is far larger than the leakage inductance of the transformers, the impedance of the distribution network can be ignored. Then, (7) is identical with (5). That is to say, by selecting  $u_q$  to be  $u_{bc}$  and setting the transformer turn ratio with (4), the fault current can be constrained to around zero. The residual current caused by the difference between (5) and (7) can be obtained by the equivalent circuit in Fig. 5, where  $U_{N\_res}$  is the residual voltage of the neutral voltage subtracted by  $-E_C$ . That is,

$$U_{N\_res} = -j3\omega_0 \frac{l_{lk-T1} + 3l_{lk-T2}}{Z_\Sigma} E_C \quad (8)$$

Therefore, the residual fault current can be expressed as

$$I_{res} = \frac{-j9E_C\omega_0(l_{lk-T1} + 3l_{lk-T2})}{j\omega_0(l_{lk-T1} + 3l_{lk-T2})(Z_\Sigma + 9R_f) + 3Z_\Sigma R_f} \quad (9)$$

Thus, when the residual fault current is constrained down to near zero by the proposed arc suppression device and the fault arc cannot be rekindled again. Then, the reliable SLG fault arc suppression can be achieved.

### IV. SIMULATION VERIFICATION

To confirm the feasibility of the ZVR arc-suppression device, a simulation model in PSIM for the 10kV distribution network in Fig. 1 is established.

**TABLE 2. Parameters of a typical distribution network.**

Parameter	Value
Turn ratio of $T_1(N_{p1}/N_{s1}/N_{s1})$	10.5/10.5/0.4
Turn ratio of $T_2(N_{p2}/N_{s2})$	10.5/0.4
Ground resistance $R_0$	12.7k $\Omega$
Ground capacitance $C_0$	8.36 $\mu$ F
Leakage inductance of $T_1(I_{lk-T1})$	18.39 $\mu$ H
Leakage inductance of $T_2(I_{lk-T2})$	0.4045mH
Frequency $\omega_0$	314rad/s

The main parameters of the distribution network are listed in TABLE 2. Notice that comparative situations are carried out into two groups in order to validate the theoretical analysis. First group is low-resistance SLG fault (set as 10 $\Omega$ ) happening to per-phase respectively, another group simulates the high-resistance SLG fault (set as 10k $\Omega$ ) occurring in phase A. Note that the stability margin is presented as it is easier to be observed for the permanent steady-state of the low-resistance (10 $\Omega$ ) and high-resistance (10k $\Omega$ ) ground-fault, as well as ground-fault arc in distribution network.

All the fault time points are set at  $t = 0.4s$ . To testify the relationship of  $U_f = E_X + U_n$ , ( $X = A, B$  or  $C$ ), simulation results are shown in Fig. 6–9, containing faulty phase voltage  $U_f$ , zero-sequence voltage  $U_n$  and fault phase current  $I_{xf}$ , ( $x = a, b$  or  $c$ ).

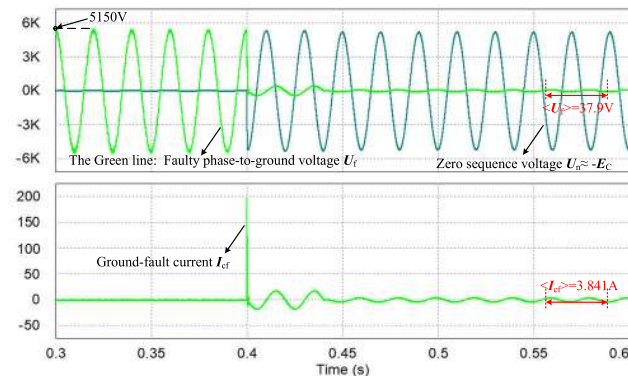


**FIGURE 6. Waveform of zero-sequence voltage and faulty phase voltage when low-resistance grounding fault occurs in phase C.**

In Fig. 6–8, the single-phase isolated transformer is accessed by turning on the multi-terminal breakers ( $S_{cn}, S_{bp}$  for Fig. 6,  $S_{an}, S_{cp}$  for Fig. 7 and  $S_{bn}, S_{ap}$  for Fig. 8) at 0.4s, to inject line-to-line voltage  $u_{bc}, u_{ca}$  and  $u_{ab}$  to the neutral point, respectively. There is a short transient change from 0.4s to 0.45s. After 0.45s, the fault-phase voltage  $U_f$  is stably suppressed to 37.9V, and the residual fault current is constrained down to 3.841A. Similar simulation results of A phase and B phase grounding fault show in Fig. 7 and Fig. 8, which demonstrates the principle mentioned in section II.

In the second group, the high-resistance (10k) SLG fault is simulated for phase A grounding fault, as shown in Fig. 9. The SLG fault still occurs at 0.4s. The transient change lasts for 0.15s. After 0.55s, the faulty phase voltage and the residual

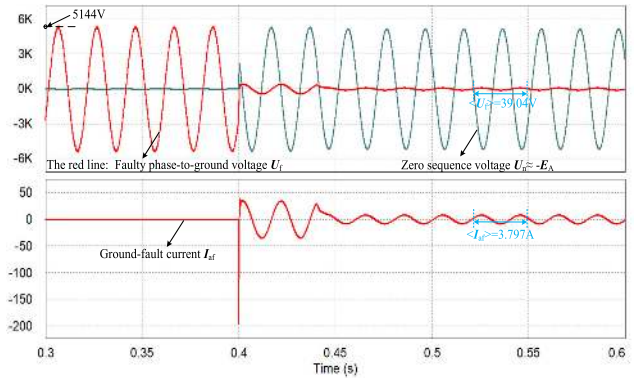


**FIGURE 7. Waveform of zero-sequence voltage and faulty phase voltage as well as ground-fault current when low-resistance grounding fault occurs in phase A.**

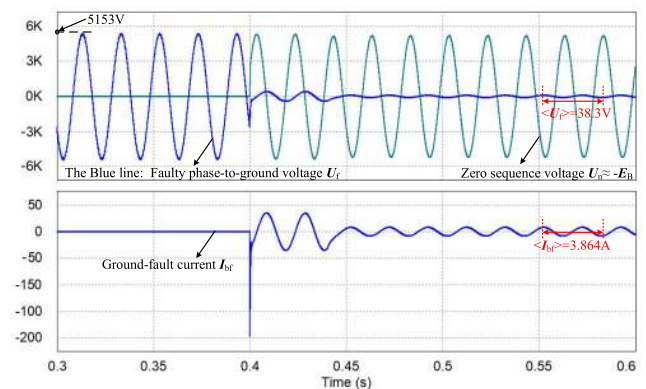


**FIGURE 8. Waveform of zero-sequence voltage and faulty phase voltage as well as ground-fault current when low-resistance grounding fault occurs in phase B.**

current are constrained down to 212.83V and 0.021A, respectively.

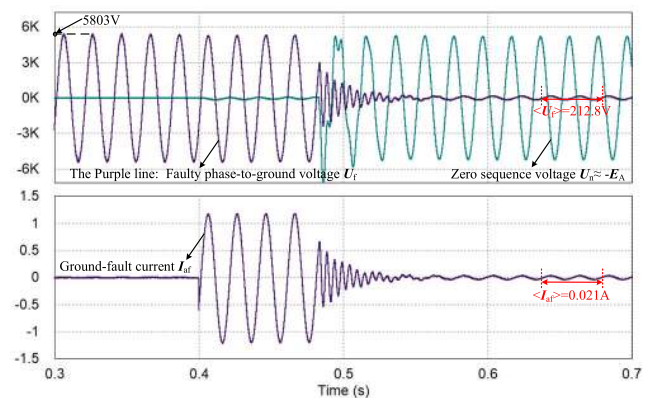


**FIGURE 9. Waveform of zero-sequence voltage and faulty phase voltage as well as ground-fault current when high-resistance grounding fault occurs in phase A.**

Further, four simulation results of Peterson coil and the proposed ZVR method are compared in Table 3, which indicates that the proposed ZVR method has better performance in capacitive current compensation.

TABLE 3. Comparative method results.

Group	Method	Residual current	Fault phase voltage	Fault resistance	Faulty phase
1 <sup>st</sup>	Peterson	6.91A	52.2V	10Ω	Phase A
	ZVR	3.797A	39.04V	10Ω	Phase A
2 <sup>nd</sup>	Peterson	6.1A	51.4V	10Ω	Phase B
	ZVR	3.864A	38.3V	10Ω	Phase B
3 <sup>rd</sup>	Peterson	6.17A	50.3V	10Ω	Phase C
	ZVR	3.841A	37.9V	10Ω	Phase C
4 <sup>th</sup>	Peterson	0.0351A	351.11V	10kΩ	Phase A
	ZVR	0.021A	212.8V	10kΩ	Phase A

TABLE 4. Experimental parameters.

Parameter	Value
Phase-to-neutral voltage $U_X$	220V
Grid frequency $f$	50Hz
Nominal phase-to-ground resistance	10kΩ
Nominal phase-to-ground capacitance	8.36μF
Ground-fault resistance	100Ω, 1kΩ, 10kΩ
Isolated transformer capacity	500kVA
Zigzag grounding transformer capacity	500kVA

The implementation flowchart of the proposed arc suppression method is shown in Fig. 10. First, by measuring all the parameter in need to detect the SLG fault, the faulty phase can be identified [22]. Then turn on the corresponding multi-terminal breakers (refers to TABLE 1) for generating the line-to-line voltage  $u_q$  to quickly control zero-sequence voltage  $U_N$ . With the precise adjustment in turn ratio of  $N_{p2}$ , ( $N_{p2} = N_{p1} * N_{s2} / N_{s1}$ ), zero-sequence voltage can be altered to be the opposite of the faulty phase supply voltage. After certain delay, if the  $U_N$  is less than 5% of the nominal phase voltage, then the device stays put for further instruction. If not, the step should be backing-out to go through the whole process of the arc suppression movement one more time. Finally, the system realizes reliable arc suppression in SLG fault.

V. EXPERIMENT VERIFICATION

To verify the proposed arc suppression system practically, a 10 kVA prototype is developed in laboratory, where 10kVA is converted by 380V power supply with a boosting transformer, shown in Fig. 11. The capacity of transformer  $T_2$  is 100kVA. The experimental parameters are listed in TABLE 4. Then, 30% of the phase-to-ground parameters in TABLE 2 represents the value of load. Thus, experiment analyses focus on the dynamic and permanent steady-state performance, the operation and parameter design follow the principle in section II.

The nominal phase-to-ground capacitance have been set in the experiment. Single-phase on-load voltage regulator (shown in Fig. 11) imitates the effect of the ZVR arc suppression device. Following the theoretical analyses in section II, the experiments are carried out into three groups, with ground-faults setting as 100Ω, 1kΩ and 10kΩ. Experiment results demonstrate the adaptability of the ZVR method.

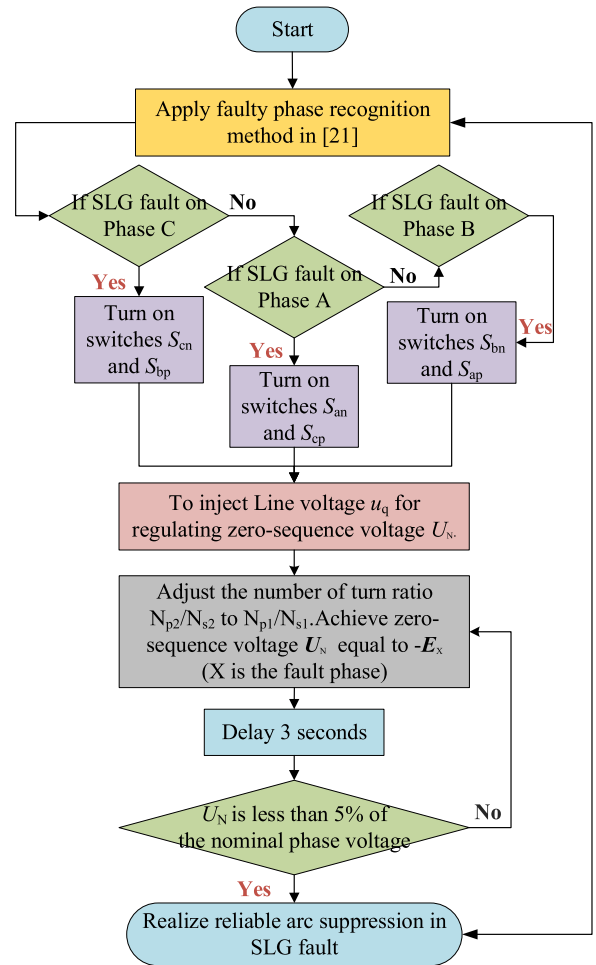


FIGURE 10. Implementation flowchart of ZVR device when SLG fault occurs in distribution network.

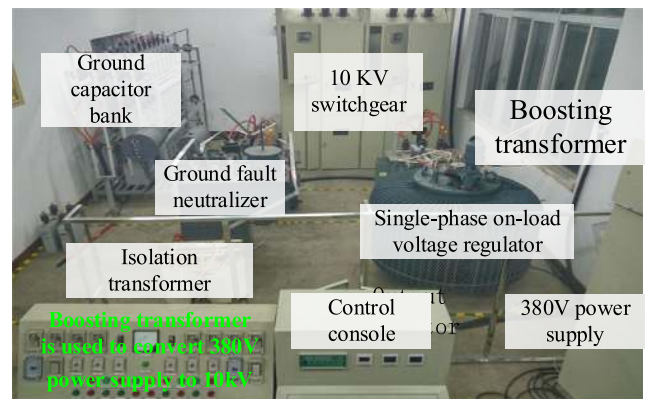
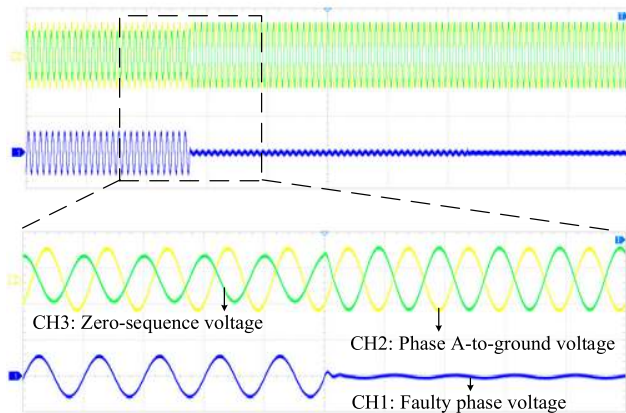


FIGURE 11. Experimental system.

Fig. 12–14 give the neutral-to-ground voltage ( $U_N$ ), phase A positive sequence voltage ( $E_A$ ) and the fault phase voltage ( $U_f$ ) when the fault resistances are 100Ω, 1kΩ and 10kΩ respectively. Again, the ZVR device is activated after the SLG fault occurs in Fig. 12–14. As shown in Fig. 12, when the 100Ω SLG fault occurs, the single-phase on-load voltage regulator regulates the zero-sequence voltage at the neutral point. Then, the fault phase voltage is constrained down to

**TABLE 5.** Experimental peak value in permanent steady state.

Group	Residual fault current	Fault phase voltage	ZVR time	Fault resistance
1 <sup>st</sup>	2.01A	20.11V	0.06s	100Ω
2 <sup>nd</sup>	0.066A	66.3V	0.12s	1kΩ
3 <sup>rd</sup>	0.0215A	214.8V	0.15s	10kΩ



**FIGURE 12.** Experiment result under a SLG fault on phase A ( $R_f = 100\Omega$ ). CH1: Faulty phase voltage (1895 V/div, t:0.1s/div) CH2: phase A supply voltage (1895 V/div, t:0.1s/div) CH3: zero-sequence voltage (1895V/div, t:0.1 s/div).

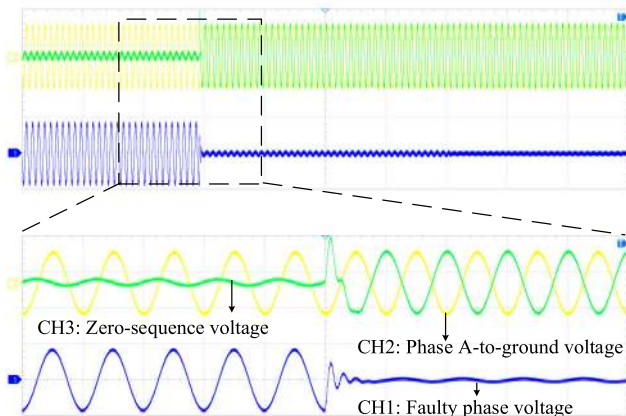
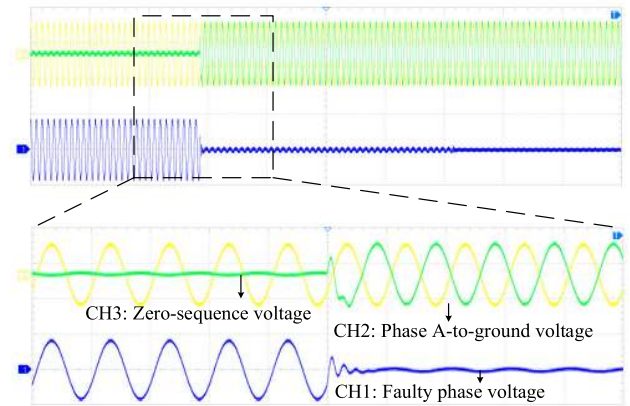


**FIGURE 13.** Experiment result under a SLG fault on phase A ( $R_f = 1k\Omega$ ). CH1: Faulty phase voltage (1895 V/div, t:0.1s/div) CH2: phase A supply voltage (1895 V/div, t:0.1s/div) CH3: zero-sequence voltage (1895V/div, t:0.1 s/div).

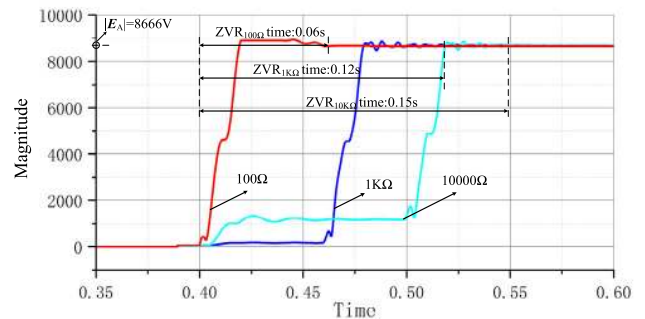
20.11 V. In Fig. 13, the whole progress of ZVR arc suppression takes only 0.12s, with constrained faulty voltage of 57.81V. The final experiment result shows that the faulty voltage in Fig. 14 is constrained down to 214.8V.

TABLE 5 records the experimental peak values of three experiment groups, and shows the adaptability of the ZVR device in either low-resistance ground-fault (i.e.,100Ω), or high-resistance ground-fault (1k–10kΩ). Thus, the proposed device can realize reliable arc suppression in SLG fault.

The correctness in the proposed method is accurately verified by principal analysis, the simulation analysis graph, data and the experimental verification.



**FIGURE 14.** Experiment result under a SLG fault on phase A ( $R_f = 10k\Omega$ ). CH1: Faulty phase voltage (1895 V/div, t:0.1s/div) CH2: phase A supply voltage (1895 V/div, t:0.1s/div) CH3: zero-sequence voltage (1895V/div, t:0.1 s/div).



**FIGURE 15.** Magnitude trajectory of zero-sequence voltage adopting ZVR device under different ground-faults.

The whole courses of zero-sequence voltage regulation in three experiments are presented in Fig. 15, where records three trajectories of the adjusted zero-sequence voltage. (100Ω, 1kΩ and 10kΩ ground-fault being suppressed, respectively). Process times of ZVR device under different ground-faults are presented. The ZVR magnitude trajectories are clearly shows that three groups of zero-sequence voltage are eventually regulated to the same magnitude value (8666V).

According to the principle in section II, if zero-sequence voltage is regulated to the opposite of the faulty phase supply voltage, ( $U_f = E_X + U_n$ ), then the ground-fault voltage can be constrained down to zero, and reliable arc suppression can be achieved.

Meanwhile, different characteristics are recorded in TABLE 6 to better present great performance of the proposed ZVR device.

Through the comparison with conventional methods, the proposed method has the advantages of low-cost and low controlling complexity. Because the proposed method doesn't need to detect the ground parameters or capacitive current for arc suppression, it is easy to operate in practice. Therefore, the correctness of this proposed ZVR arc suppression device is accurately verified by principal analysis, simulation analysis graph, data, and the experimental verification. Thus,

**TABLE 6. Comparative characteristics in different arc suppression methods.**

Types	Detection complexity	Reliability	Cost	Control complexity
Peterson	YES	HIGH	MIDDLE	HIGH
Voltage-based ASD	NO	LOW	HIGH	HIGH
Fault-transfer Switch	NO	HIGH	VERY HIGH	LOW
ZVR method	NO	MEDDLE	VERY LOW	LOW

the proposed method has great performance of reliability, adaptability and accuracy.

## VI. CONCLUSION

This paper, focusing on SLG fault problem, proposes a zero-sequence regulation-based arc suppression device. The proposed ZVR arc suppression device includes the zigzag grounding transformer, multi-terminal breakers and the single-phase isolation transformer. Rigorous researches on neutral ungrounded system of distribution network and strict principle of zero-sequence regulation method are analyzed. Several ground-fault conditions are simulated and experiments under same conditions are made, in order to demonstrate the correctness of the proposed ZVR method.

Peterson coils, voltage-based ASD, fault-transfer switch and the proposed ZVR method are comparatively analyzed in detection complexity, reliability, controlling complexity and cost. It illustrates that the proposed ZVR device is cost-effective without the need of Peterson coil and using fewer number of electronic components. It has excellent reliability with reduced controlling complexity, realizing desired arc suppression effectiveness.

Further study includes experiment in prototype of ground-fault arc and field test on the sensibility of the proposed method. In sum, the proposed ZVR device is cost-effective and it is easy to operate.

## REFERENCES

- [1] W. Qiu, M. F. Guo, G. J. Yang, and Z. Y. Zheng, "Model-predictive-control-based flexible arc-suppression method for earth fault in distribution networks," *IEEE Access*, vol. 7, pp. 16051–16065, 2019.
- [2] P. S. Moses, M. A. S. Masoum, and H. A. Toliyat, "Impacts of hysteresis and magnetic couplings on the stability domain of ferroresonance in asymmetric three-phase three-leg transformers," *IEEE Trans. Energy Convers.*, vol. 26, no. 2, pp. 581–592, Jun. 2011.
- [3] X. Wang, H. Zhang, F. Shi, Q. Wu, V. Terzija, W. Xie, and C. Fang, "Location of single phase to ground faults in distribution networks based on synchronous transients energy analysis," *IEEE Trans. Smart Grid*, vol. 11, no. 1, pp. 774–785, Jan. 2020.
- [4] W. Peng, C. Baichao, T. Cuihua, B. Sun, M. Zhou, and J. Yuan, "A novel neutral electromagnetic hybrid flexible grounding method in distribution networks," *IEEE Trans. Power Del.*, vol. 32, no. 3, pp. 1350–1358, Jun. 2017.
- [5] *IEEE Recommended Practice for Grounding of Industrial and Commercial Power Systems*, IEEE Standard 142-2007 (Revision of IEEE Standard 142-1991), Nov. 2007, pp. 1–225.
- [6] S. Ouyang, J. Liu, Y. Yang, X. Chen, S. Song, and H. Wu, "Control strategy for Arc-Suppression-Coil-Grounded star-connected power electronic transformers," *IEEE Trans. Power Electron.*, vol. 34, no. 6, pp. 5294–5311, Jun. 2019.

- [7] A. Cerretti, F. M. Gatta, A. Geri, S. Lauria, M. Maccioni, and G. Valtorta, "Ground fault temporary overvoltages in MV networks: Evaluation and experimental tests," *IEEE Trans. Power Del.*, vol. 27, no. 3, pp. 1592–1600, Jul. 2012.
- [8] R. Burgess and A. Ahfock, "Minimising the risk of cross-country faults in systems using arc suppression coils," *IET Gener., Transmiss. Distrib.*, vol. 5, no. 7, pp. 703–711, Jul. 2011.
- [9] W. Wang, X. Zeng, L. Yan, X. Xu, and J. M. Guerrero, "Principle and control design of active ground-fault arc suppression device for full compensation of ground current," *IEEE Trans. Ind. Electron.*, vol. 64, no. 6, pp. 4561–4570, Jun. 2017.
- [10] X. Zeng, Y. Xu, and Y. Wang, "Some novel techniques for insulation parameters measurement and petersen-coil control in distribution systems," *IEEE Trans. Ind. Electron.*, vol. 57, no. 4, pp. 1445–1451, Apr. 2010.
- [11] W. Wang, L. Yan, B. Fan, and X. Zeng, "Control method of an arc suppression device based on single-phase inverter," in *Proc. Int. Symp. Power Electron., Electr. Drives, Autom. Motion (SPEEDAM)*, Jun. 2016, pp. 929–934.
- [12] P. Toman, M. Paar, and J. Orsagova, "Possible solutions to problems of voltage asymmetry and localization of failures in MV compensated networks," in *Proc. IEEE Lausanne Power Tech*, Jul. 2007, pp. 1758–1763.
- [13] S. K. Dash, G. Panda, P. K. Ray, and S. S. Pujari, "Realization of active power filter based on indirect current control algorithm using xilinx system generator for harmonic elimination," *Int. J. Electr. Power Energy Syst.*, vol. 74, pp. 420–428, Jan. 2016.
- [14] M. Janssen, S. Kraemer, R. Schmidt, and K. Winter, "Residual current compensation (RCC) for resonant grounded transmission systems using high performance voltage source inverter," in *Proc. IEEE PES Transmiss. Distrib. Conf. Expo.*, vol. 2, Dallas, TX, USA, Sep. 2003, pp. 574–578.
- [15] A. De Conti, V. C. Oliveira, P. R. Rodrigues, F. H. Silveira, J. L. Silvino, and R. Alipio, "Effect of a lossy dispersive ground on lightning overvoltages transferred to the low-voltage side of a single-phase distribution transformer," *Electr. Power Syst. Res.*, vol. 153, pp. 104–110, Dec. 2017.
- [16] W. Wang, L. Yan, X. Zeng, B. Fan, and J. M. Guerrero, "Principle and design of a single-phase inverter-based grounding system for neutral-to-ground voltage compensation in distribution networks," *IEEE Trans. Ind. Electron.*, vol. 64, no. 2, pp. 1204–1213, Feb. 2017.
- [17] J. Meng, W. Wang, X. Tang, and X. Xu, "Zero-sequence voltage trajectory analysis for unbalanced distribution networks on single-line-to-ground fault condition," *Electr. Power Syst. Res.*, vol. 161, pp. 17–25, Aug. 2018.
- [18] Z. Xu, B. Li, S. Wang, S. Zhang, and D. Xu, "Generalized single-phase harmonic state space modeling of the modular multilevel converter with zero-sequence voltage compensation," *IEEE Trans. Ind. Electron.*, vol. 66, no. 8, pp. 6416–6426, Aug. 2019.
- [19] X. Li, J. Han, Y. Sun, M. Su, J. Lin, S. Xie, and S. Huang, "A generalized design framework for neutral point voltage balance of three-phase vienna rectifiers," *IEEE Trans. Power Electron.*, vol. 34, no. 10, pp. 10221–10232, Oct. 2019.
- [20] H. Nouri and M. M. Alamuti, "Comprehensive distribution network fault location using the distributed parameter model," *IEEE Trans. Power Del.*, vol. 26, no. 4, pp. 2154–2162, Oct. 2011.
- [21] B. Fan, G. Yao, W. Wang, X. Yang, H. Ma, K. Yu, C. Zhuo, and X. Zeng, "Faulty phase recognition method based on phase-to-ground voltages variation for neutral ungrounded distribution networks," *Electr. Power Syst. Res.*, vol. 190, Jan. 2021, Art. no. 106848.



**BISHUANG FAN** (Member, IEEE) received the bachelor's degree from Changsha Traffic University, Changsha, China, in 2002, the master's degree from the Changsha University of Science and Technology, Changsha, in 2007, and the Ph.D. degree from Central South University, Changsha, in 2014. In 2016, he was a Visiting Scholar with the Power Electronics Laboratory, Department of Electrical Engineering and Computer Science, The University of Tennessee, Knoxville, TN, USA.

Since 2015, he has been an Associate Professor with the School of Electrical and Information Engineering, Changsha University of Science and Technology. His current research interest includes power conversion technologies.



**GANZHOU YAO** (Student Member, IEEE) was born in Guangdong, China, in 1995. He received the B.S. degree in electrical engineering and automation from the Chengnan College, Changsha University of Science and Technology, Hunan, China, in 2014, where he is currently pursuing the M.S. degree in electrical engineering.

His research interest includes power electronic technology in grounding systems.



**KUN YU** (Member, IEEE) received the M.S. degree from the Changsha University of Science and Technology, in 2014, and the Ph.D. degree from the Huazhong University of Science and Technology, Wuhan, in 2017. He is currently a Lecturer with the Changsha University of Science and Technology. His research interest includes power system protection and control.



**XIANGJUN ZENG** (Senior Member, IEEE) received the B.S. degree in electrical engineering from Hunan University, Changsha, China, in 1993, the M.S. degree in electrical engineering from Wuhan University, Wuhan, China, in 1996, and the Ph.D. degree in electrical engineering from the Huazhong University of Science and Technology, Wuhan, in 2001.

He was a Postdoctoral Fellow with Xuji Relay Company and The Hong Kong Polytechnic University, and a Visiting Professor with Nanyang Technological University, Singapore. He is currently a Professor and the Dean of the School of Electrical and Information Engineering, Changsha University of Science and Technology, Changsha. His research interest includes real-time computer applications in power systems control and protection.



**WEN WANG** (Member, IEEE) received the B.S. and Ph.D. degrees in electrical engineering from Hunan University, Changsha, China, in 2008 and 2013, respectively. In 2016, he was a Guest Researcher with the Department of Energy Technology, Aalborg University, Aalborg, Denmark. Since 2018, he has been an Associate Professor with the School of Electrical and Information Engineering, Changsha University of Science and Technology, Changsha. His current research interests include power electronics and its application in power systems, and grounding methods in distribution networks.



**CHAO ZHUO** received the M.S. degree from the Changsha University of Science and Technology, in 2011, and the Ph.D. degree from Guangxi University, Nanning, in 2020. He currently holds a postdoctoral position with the Changsha University of Science and Technology. His research interest includes power system protection and control.



**JOSEP M. GUERRERO** (Fellow, IEEE) received the B.S. degree in telecommunications engineering, the M.S. degree in electronics engineering, and the Ph.D. degree in power electronics from the Technical University of Catalonia, Barcelona, Spain, in 1997, 2000, and 2003, respectively.

Since 2011, he has been a Full Professor with the Department of Energy Technology, Aalborg University, Aalborg, Denmark, where he is responsible for the Microgrid Research Program. His research interests include power electronics, distributed energy-storage systems, hierarchical and cooperative control, energy management systems, smart metering, and the Internet of Things for ac/dc microgrid clusters and islanded microgrids; recently, there has been a special focus on maritime microgrids for electrical ships, vessels, ferries, and seaports.

Dr. Guerrero is an Associate Editor of the IEEE TRANSACTIONS ON POWER ELECTRONICS, IEEE TRANSACTIONS ON INDUSTRIAL ELECTRONICS, and *IEEE Industrial Electronics Magazine*, and an Editor of the IEEE TRANSACTIONS ON SMART GRID and IEEE TRANSACTIONS ON ENERGY CONVERSION.

• • •